Proceedings of the 9th U.S. National and 10th Canadian Conference on Earthquake Engineering
Compte Rendu de la 9ième Conférence Nationale Américaine et
10ième Conférence Canadienne de Génie Parasismique
July 25-29, 2010, Toronto, Ontario, Canada • Paper No 619

OPTIMUM SELECTION OF ISOLATOR PROPORTIES FOR EFFECTIVE MITIGATION OF SEISMIC RISK FOR BRIDGES

M.Karalar[1] and M.Dicleli[2]

ABSTRACT

In this study, closed form equations as functions of the isolator, bridge and ground motion properties are formulated to calculate the optimum characteristic strength, Q_d and post-elastic stiffness, k_d, of the isolator to minimize the maximum isolator displacement (MID) and force (MIF) for seismic isolated bridges (SIBs). This formulation required more than 13000 nonlinear time history analyses of simplified SIB models. The analyses results revealed that the optimum Q_d and k_d are highly dependent on the site soil conditions and peak ground acceleration of the ground motion.

Introduction

The force-displacement hysteresis of most commercially available isolators is generally idealized as bilinear for design purposes. A typical bilinear force-displacement hysteresis of an isolator and a typical isolated bridge substructure are shown in Figs. 1(a) and (b). In the figures, Q_d is the characteristic strength, k_u is the elastic stiffness, k_d is the post-elastic stiffness, F_y and u_y are respectively the yield force and displacement and F_i and u_i are respectively the maximum (or design) force and displacement of the isolator. The characteristic strength, Q_d and the post-elastic stiffness, k_d, are the main isolator parameters that affect the behavior of a SIB (Dicleli and Buddaram 2006). Thus, the optimal selection of these isolator parameters based on minimizing the MID and MIF will result in an economical design of the SIB. Several research studies have been conducted to identify the optimal characteristic properties of isolators or yielding systems for the seismic design of structures (Veletsos et al. 1965, Park and Otsuka 1999, Iemura et al. 2007). However, none of these research studies provide simple yet effective equations to calculate the optimal isolator properties. Therefore, it is clear that closed form equations as functions of the properties of the bridge, isolator and frequency characteristics and intensity of actual ground motions are still needed to obtain the optimum values of the isolator characteristic parameters, Q_d and k_d based on minimizing the MID and MIF. Such equations may be used by the bridge engineering community to select proper values of Q_d and k_d for the economical seismic design of SIBs. Accordingly, the main objective of this study is to formulate closed form equations as functions of the isolator, bridge and ground motion properties to calculate the isolator properties, Q_d, k_d, to minimize the MID and MIF.

[1]Graduate Research Assistant, Department of Engineering Sciences, Middle East Technical University, Ankara, Turkey, E-mail: memduh@metu.edu.tr
[2]Professor, Department of Engineering Sciences, Middle East Technical University, Ankara, Turkey, E-mail: mdicleli@metu.edu.tr,.

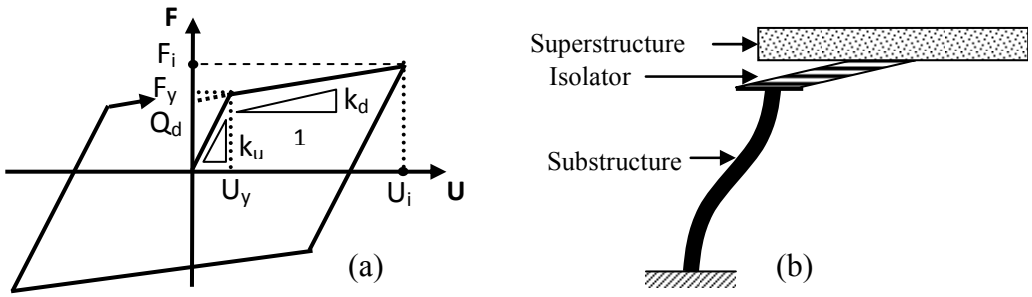

Figure 1. (a) Idealized hysteresis loop of a typical isolator, (b) Typical seismic-isolated bridge substructure

Ground Motions and Parameters Considered

Two sets of ground motions are used. The first set involves a suite of 15 earthquakes with A_p/V_p ratios (represent their dominant frequency and energy content) ranging between 5.50 s^{-1} and 21.5 s^{-1} presented in Table 1 (No.: 1-15). These ground motions are used for the formulation of the optimum values of Q_d and k_d. The second set involves a suite of five earthquakes with A_p/V_p ratios ranging between 4.70 s^{-1} and 23.6 s^{-1} presented also in Table 1 (No.: 16-20). These ground motions are used for the verification of the equations developed to calculate the optimum values of Q_d and k_d. Several parameters are considered for the sensitivity analyses to study the effect of the bridge, isolator and ground motion properties on the optimum values of Q_d and k_d. The parameters that affect the optimum values of Q_d and k_d are then used in the optimization procedure. The parameters that are used in the sensitivity analyses are categorized into three groups as those representing the bridge, isolator and ground motion properties. The bridge properties are represented by the superstructure mass, m, substructure stiffness, k_s and structural or supplemental damping, ζ.

The superstructure mass tributary to a typical isolator is taken as a constant equal to 204 tons (2000 kN weight). The substructure stiffness is varied between 200 kN/cm (very flexible) and 6400 kN/cm (very stiff). This stiffness range corresponds to 10 to 320 times the 20 kN/cm post elastic stiffness of the isolator used in the analyses while studying the effect of the substructure stiffness on the optimum values of Q_d and k_d. The structural and/or supplemental damping is varied between 0% and 8% of critical. The isolator's elastic stiffness is not considered as a parameter in this study since its effect on the performance of SIBs has been found to be negligible earlier by Dicleli and Buddaram (2006).

Dimensionles Parameters Used in the Development of the Equations

Makris and Black (2004a, 2004b) proposed four dimensionless terms to describe the response of a structural system with bilinear force-deformation relationship in relation to the characteristics of a pulse type excitation with a period, T_p. Two of the proposed terms; $\Pi_2=Q_d/mA_p$, and $\Pi_4= T_d/T_p$, are used in this study to represent the analyses results where T_d is the period of the bridge based on the post-elastic stiffness, k_d, of the isolator and all the other variables are as described before. Since seismic ground motions with various frequency characteristics are considered in the presented study, the term, T_p, is replaced by the dominant period of the ground motion given as $T_g= 2\pi/(A_p/V_p)$ (Kramer 1996).

Table 1. Important features of the earthquake records used in the analyses.

No	Earthquake	Station / Component	A_p/V_p (1/s)
1	San Fernando, 1971	8244 Orion Blvd. / 180°	5.5
2	Imperial Valley, 1940	El Centro / 180°	5.8
3	Loma Prieta, 1989	Oakland Outer Wharf / 0°	6.1
4	Loma Prieta, 1989	Oakland Outer Wharf / 270°	7.2
5	Northridge, 1994	Arleta and Nordhoff Fire Station / 90°	8.4
6	Kern County, 1952	Taft Lincoln Tunnel / 69°	9.7
7	Imperial Valley, 1940	El Centro / 270°	10.6
8	Santa Barbara, 1978	283 Santa Barbara Courthouse / 222°	12.2
9	Coalinga, 1983	36227 Parkfield - Cholame 5W / 270°	13.4
10	Northridge, 1994	Santa Monica City Hall Grounds / 0°	14.6
11	Whitter Narrows, 1987	24401 San Marino, SW Academy / 360°	15.6
12	Whitter Narrows, 1987	90079 Downey Birchdale / 90°	17.4
13	San Fernando, 1971	Pacoima Dam. / 196°	18.4
14	Northridge, 1994	Santa Monica City Hall Grounds / 90°	20.7
15	Parkfield, 1966	Cholame, Shandon / 40°	21.5
16	Borrego Mount., 1968	Hollywood Storage Lot / 180°	4.7
17	Kobe, 1995	FUK / 0°	7.7
18	Friuli, Italy, 1976	Conegliano / 0°	13.6
19	NW California, 1941	Ferndale City Hall / 45°	16.7
20	Morgan Hill, 1984	San Francisco Int. Airport, / 90°	23.6

Optimization Procedure

The calculation of the optimum values of Q_d and k_d to minimize the MIF and MID consists of three sets of analyses. The first two sets of analyses are performed to obtain the optimum values of Q_d to minimize the MIF and MID respectively. The third set of analyses is performed to obtain the optimum values of k_d to minimize the MID.

To calculate the optimum values of Q_d to minimize the MIF, first, the MIF is determined for a wide range of presumed Q_d values. Next, the bisection search method is used between the data points before and after the apparent minimum value of MIF within the MIF-Q_d plot, to determine the actual minimum MIF and the corresponding optimal value of Q_d. This procedure is repeated for the range of parameters and ground motions considered in this study to obtain a wide range of data giving the optimal Q_d values. Similar procedures are also used to obtain the optimum values of Q_d and k_d corresponding to minimum MID.

Effect of Various Parameters on Optimum Q_d

In this section, sensitivity analyses are conducted to identify the parameters that affect the optimum value of Q_d, based on minimizing the MIF and MID. The bridge, isolator and ground motion parameters used in the analyses are; m=204 ton (W=2000 kN), ζ=0, k_u=200 kN/cm, k_d=20 kN/cm, k_s/k_d=160, A_p=0.6g and A_p/V_p=5.8, 12.2 and 21.5 s^{-1} (i.e. the analyses are repeated for

three ground motions). In the sensitivity analyses, while the parameter under consideration is varied, the rest of the parameters are assigned the values reported above.

Effect of Peak Ground Acceleration

In this section, the effect of the peak ground acceleration, A_p on the optimum value of Q_d is investigated by varying the peak ground acceleration between 0.1g and 1.0g. The sensitivity analyses results are presented in Figs. 2(a) and (b) for three ground motions with A_p/V_p =5.8, 12.2 and 21.5 s^{-1} in the form of optimum Q_d versus A_p plots based on minimizing the MIF and MID respectively. As observed from the figures, the optimum value of Q_d is linearly proportional to A_p. Knowing this, the optimum value of Q_d is normalized with respect to mA_p as suggested by Makris and Black (2004a) and re-plotted in Figs. 2(c) and (d). As observed from the figures, the Q_d/mA_p ratio is independent of the peak ground acceleration, A_p. Thus, for the remainder of the study, the peak ground acceleration is not considered as an independent parameter. Instead the Q_d/mA_p ratio is used in the optimization procedure. The dimensionless term, Q_d/mA_p, is also used in the presentation of the analyses results for the remainder of the study.

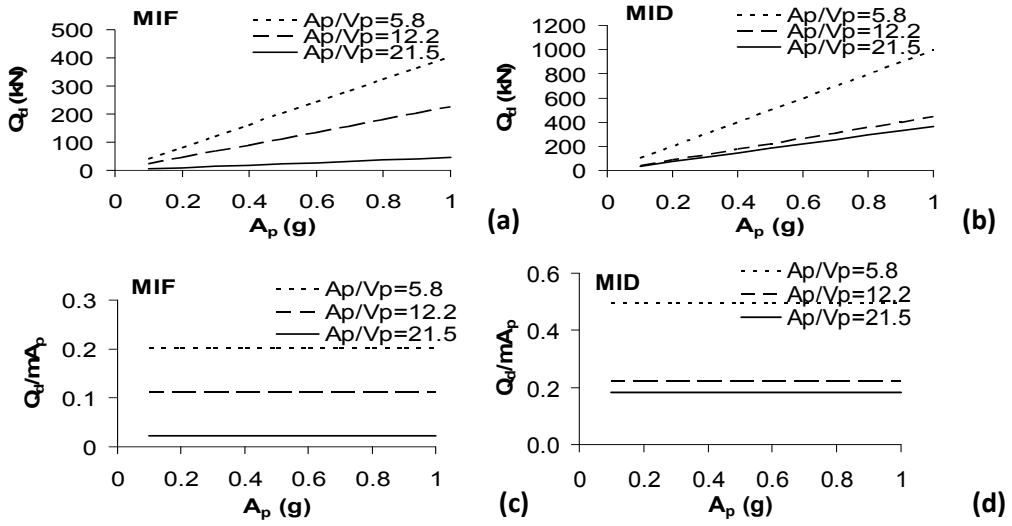

Figure 2. Effect of various parameters on optimum Q_d (a) A_p for MIF (b) A_p for MID, (c) A_p for MIF using Q_d/mA_p ratio, (d) A_p for MID using Q_d/mA_p ratio.

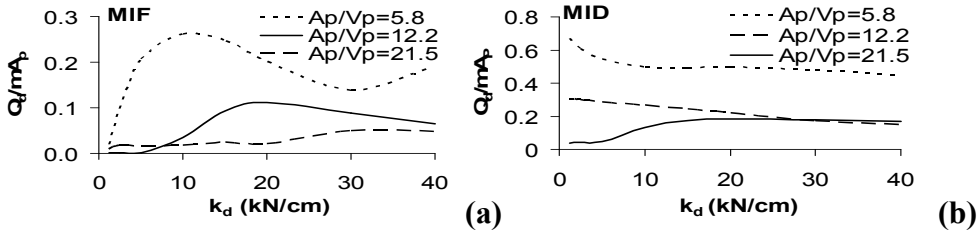

Figure 3. Effect of various parameters on optimum Q_d (a) k_d for MIF, (b) k_d for MID

Effect of A_p/V_p Ratio of Ground Motion Effect

In this section, the effect of the A_p/V_p ratio of the ground motion on the optimum value of Q_d is investigated. The sensitivity analyses results presented in Figs. 2(a), (b), (c) and (d) reveal that, the optimum value of Q_d/mA_p ratio or Q_d is highly dependent on the A_p/V_p ratio of the ground motion. That is, for each A_p/V_p ratio, a different relationship between Q_d and A_p is obtained. In general, the sensitivity analyses results revealed that the optimum value of Q_d increases as the A_p/V_p ratio of the ground motion decreases (Figs. 2(a) and (b)). Thus, the A_p/V_p ratio of the ground motion must be included as a parameter in the development of closed form equations to calculate the optimum values of Q_d based on minimizing the MIF and MID.

Effect of Post-Elastic Stiffness of the Isolator

In this section, the effect of the post-elastic stiffness, k_d, of the isolator on the optimum value of Q_d is investigated. For this purpose, NLTH analyses of simplified structural models of SIBs with isolators having k_d ranging between 1.25 and 40 kN/cm are conducted for three ground motions with A_p/V_p = 5.8, 12.2 and 21.5 s^{-1} scaled to A_p= 0.6g to determine the optimum values of Q_d based on minimizing the MIF and MID. The analyses results are presented in Figs. 3(a) and (b). As observed from the figures, the optimum Q_d/mA_p ratio varies as a function of k_d. Thus, k_d must be included as a parameter in the development of closed form equations to calculate the optimum values of Q_d based on minimizing the MIF and MID.

Effect of Structural/Supplemental Damping

In this section, the effect of structural/supplemental damping on the optimum value of Q_d is investigated. For this purpose, NLTH analyses of simplified structural models of SIBs with structural/supplemental damping ratios ranging between 0% and 7% are conducted for three ground motions with A_p/V_p= 5.8, 12.2 and 21.5 s^{-1} scaled to A_p=0.6g to determine the optimum values of Q_d based on minimizing the MIF and MID. The analyses results are presented in Figs. 4(a) and (b). As observed from the figures, the optimum Q_d/mA_p ratio varies as a function of the damping ratio. Thus, damping ratio must be included as a parameter in the development of closed form equations to calculate the optimum values of Q_d based on minimizing the MIF and MID.

Effect of Substructure Stiffness

In this section, the effect of the substructure stiffness on the optimum value of Q_d is investigated by changing, in the structural model, the ratio, ks/kd, of the lateral stiffness of the substructure to the post-elastic stiffness of the isolator between 10 (very flexible) and 320 (very stiff). The analyses results are presented in Fig. 4(c) and (d). As observed from the figures, the optimum Q_d/mA_p ratio or Q_d does not vary as a function of k_s/k_d (i.e. the curves remain nearly flat for the range of k_s/k_d ratios considered) except for the cases where the substructure is very flexible (k_s/k_d < 40).

Effect of Various Parameters on Optimum k_d

In this section, the effect of various parameters on the optimum value of k_d, based on minimizing the MID, is investigated via sensitivity analyses. The bridge, isolator and ground motion parameters used in the analyses are; m=204 ton (W=2000 kN), ζ=0, k_u=200 kN/cm, Q_d=100 kN, k_s =3200 kN/cm, A_p=0.6g and A_p/V_p=5.8, 12.2 and 21.5 s^{-1} (i.e. the analyses are repeated for three ground motions). In the sensitivity analyses, while the parameter under consideration is varied, the rest of the parameters are assigned the values reported above. The sensitivity analyses results for each parameter are given below.

Effect of Peak Ground Acceleration and Characteristic Strength

As discussed earlier, the dimensionless term, Q_d/mA_p, represents the ratio of the characteristic strength of the isolator to the seismic inertial force of a rigid bridge superstructure and eliminates the need for considering the peak ground acceleration and the characteristic strength of the isolator independently. Thus, the Q_d/mA_p ratio is used in the sensitivity analyses to study the combined effects of A_p and Q_d on the optimum value of k_d. The analyses results are presented in Figs 5(a) and for three ground motions with A_p/V_p =5.8, 12.2 and 21.5 s^{-1} in the form of optimum k_d versus Q_d/mA_p plots based on minimizing the MID. As observed from the figure, the optimum value of k_d varies as a function of the Q_d/mA_p ratio. Thus, the Q_d/mA_p ratio must be included as a parameter in the development of the closed form equation to calculate the optimum values of k_d based on minimizing the MID.

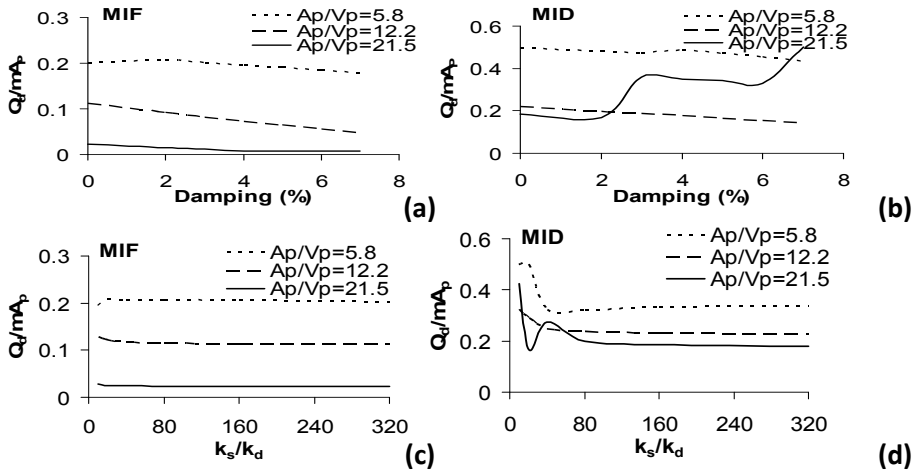

Figure 4. Effect of various parameters on optimum Q_d (a) Damping for MIF, (b) Damping for MID (c) Substructure stiffness for MIF, (d) Substructure stiffness for MID.

Effect of A_p/V_p Ratio of Ground Motion

In this section, the effect of the A_p/V_p ratio of the ground motion on the optimum value of k_d is investigated by varying the A_p/V_p ratio between 5.5 and 21.5 s^{-1} while keeping the other parameters constant. The sensitivity analyses results are presented in Fig. 5(b) in the form of an optimum k_d versus A_p/V_p ratio plot based on minimizing the MID. As observed from the figure, the optimum value of kd is highly dependent on the A_p/V_p ratio of the ground motion. In fact, the optimum value of k_d increases as the A_p/V_p ratio of the ground motion decreases. Thus, the A_p/V_p

ratio of the ground motion must be included as a parameter in the development of closed form equations to calculate the optimum values of k_d based on minimizing the MID.

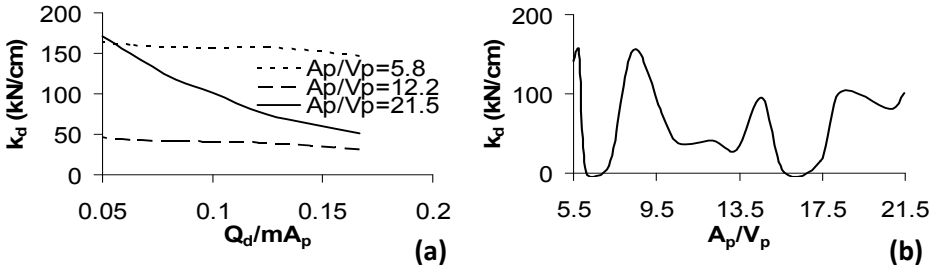

Figure 5. Effect of various parameters on optimum k_d based on minimizing the MID (a) Q_d/mA_p ratio (b) A_p/V_p ratio.

Effect of Structural/Supplemental Damping

In this section, the effect of structural/supplemental damping on the optimum value of k_d is investigated. For this purpose, NLTH analyses of simplified structural models of SIBs with structural/supplemental damping ratios ranging between 0% and 8% are conducted for three ground motions with A_p/V_p =5.8, 12.2 and 21.5 s^{-1} scaled to A_p = 0.6g to determine the optimum values of k_d based on minimizing the MID. The analyses results are presented in Fig. 6(a). As observed from the figures, the optimum value of k_d does not vary significantly as a function of the damping ratio. Thus, damping ratio need not be included as a parameter in the development of closed form equations to calculate the optimum values of k_d based on minimizing the MID.

Effect of Substructure Stiffness

In this section, the effect of the substructure stiffness on the optimum value of k_d is investigated by changing, in the structural model, the lateral stiffness, k_s, of the substructure between 200 kN/cm (very flexible) and 6400 kN/cm (very stiff). The analyses results are presented in Fig. 6(b). As observed from the figure, the optimum value of k_d does not vary as a function of k_s (i.e. the curves remain nearly flat) except for the cases where the substructure is very flexible.

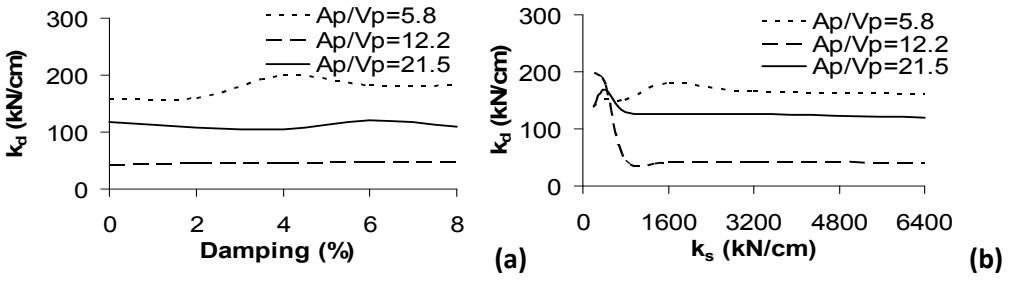

Figure 6. Effect of various parameters on optimum k_d based on minimizing the MID (a) Damping, (b) Substructure stiffness.

Formulation of the Optimum Characteristic Strength

In view of the sensitivity analyses results, the optimum values of Q_d based on minimizing the MIF and MID are calculated for a wide range of values of the parameters that are found to affect the optimum value Q_d. The analyses results for the optimum values of Q_d based on minimizing the MIF and MID are presented respectively in Fig. 7(a) and (b) in the form of Q_d/mA_p versus T_d/T_g plots. These graphs and similar plots of Q_d/mA_p versus damping are used in the formulation of the optimum Q_d based on minimizing the MIF and MID via regression analyses. Thus, the optimum $Q_{d\text{-}F}$ is obtained as;

$$Q_{d-F} = \frac{47mA_p}{50\left(\frac{T_d}{T_g}\right)^{0.7} e^{2.5\xi}} \tag{1}$$

Note that the post elastic period of the SIB, T_d and the dominant period of the ground motion, T_g, in Eq. (1) are expressed as;

$$T_d = 2\pi\sqrt{\frac{m}{k_d}} \tag{2}$$

$$T_g = \frac{2\pi}{A_p/V_p} \tag{3}$$

Substituting Eqns. (2) and (3) into Eqn. (1) and rearranging, the optimum $Q_{d\text{-}F}$ based on minimizing the MIF is obtained as;

$$Q_{d-F} = \frac{47mA_p}{50\left(\frac{m}{k_d}\right)^{0.35}\left(\frac{A_p}{V_p}\right)^{0.7} e^{2.5\xi}} \tag{4}$$

The optimum characteristic strength $Q_{d\text{-}D}$ based on minimizing the MID is also obtained as;

$$Q_{d-D} = \frac{3A_p k_d}{4\left(\frac{A_p}{V_p}\right)^{2} e^{28\xi}} \tag{5}$$

Formulation of the Optimum Post-Elastic Stiffness

In light of the sensitivity analyses results, the optimum values of k_d based on minimizing the MID are calculated for the assumed range of values of the parameters that are found to influence the optimum value of k_d. The analyses results for the optimum values of k_d based on minimizing the MID are presented in Fig. 8(a) in the form of kd versus Q_d/mA_p plot. This graph and the plot in Fig. 8(b) are used in the formulation of the optimum kd based on minimizing the

MID. The following equation that may be used to calculate the optimum values of k_d to achieve the smallest possible MID is obtained via regression analyses;

$$k_d = \left(\frac{mA_p}{Q_d}\right)^{0.34}\left[0.264\left(\frac{A_p}{V_p}\right)^2 - 7.45\left(\frac{A_p}{V_p}\right) + 72.4\right] \tag{6}$$

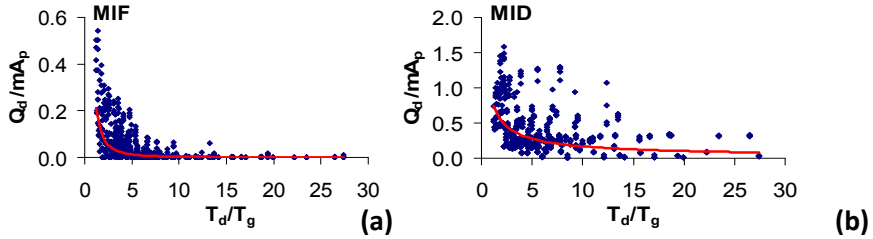

Figure 7. (a) Variation of the optimum Q_d/mA_p ratio as a function of T_d/T_g ratio based on minimizing the MIF, (b) Variation of the optimum Q_d/mA_p ratio as a function of T_d/T_g ratio based on minimizing the MID.

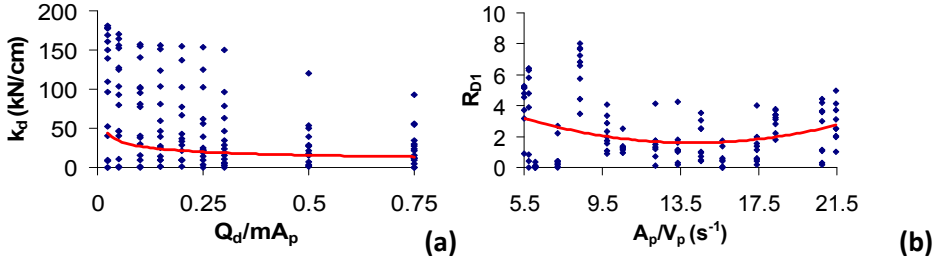

Figure 8. (a) Variation of the optimum k_d as a function of Q_d/mA_p ratio based on minimizing the MID, (b) Ratio of the optimum k_d based on minimizing the MID as a function of the A_p/V_p ratio.

Verification of the Developed Equations

The developed equations are verified using a suite of five ground motions different than those used for their development (Record # 16-20 in Table 1). The comparison of the optimum Q_d and k_d values obtained from the developed equations (Eqns. (4), (5) and (6)) with those obtained from iterative NLTH analyses are presented as a function of the A_p/V_p ratio of the ground motions in Fig.9 for various isolator properties and structural/supplemental damping ratios. As observed from the plots of Fig. 9, although some differences between the analytical and NLTH analyses results are noted at specific A_p/V_p points, in general, the overall variation of the developed equations as a function of the A_p/V_p ratio of the ground motions agrees well with the analysis results.

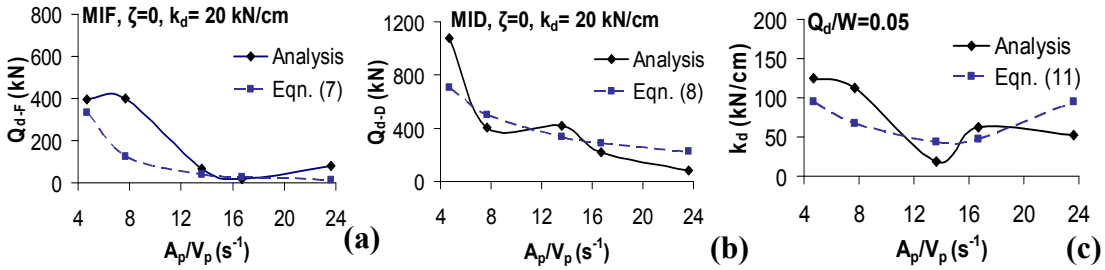

Figure 9. Comparison of the optimum isolator characteristic parameters ($Q_{d\text{-}F}$, $Q_{d\text{-}D}$, k_d) obtained from the developed equations with those obtained from NLTH analyses (a) Eqn. (4), (b) Eqn. (5), (c) Eqn. (6)

Conclusions

In this study, closed form equations as functions of the isolator, bridge and ground motion properties are formulated to calculate the optimum characteristic strength, Q_d and post-elastic stiffness, k_d, of the isolator to minimize the MID and MIF for SIBs. It is found that, the effect of the bridge substructure stiffness on the optimum Q_d and k_d and the effect of the structural/supplemental damping on the optimum k_d are negligible. The optimum Q_d and k_d are found to be highly dependent on the frequency characteristics of the ground motion and the peak ground acceleration.

References

Constantinou M. C. and Tadjbakhsh I. G., 1984.Optimum design of a base isolation system with frictional elements, *Earthquake Engineering & Structural Dynamics*, 12(2),203-214

Dicleli, M.and Buddaram S., 2006. Effect of isolator and ground motion characteristics on the performance of seismic-isolated bridges, *Earthquake Eng. and Structural Dyn*., 35(2), 233-250.

Iemura H., Taghikhany, T., Jain S. K., 2007. Optimum design of resilient sliding isolation system for seismic protection of equipments. *Bulletin of Earthquake Engineering*, 5:85–103.

Makris, N. and C. J. Black, 2004a. Dimensional analysis of rigid-plastic and elastoplastic structures under pulse type excitations. *Journal of Engineering Mechanics, ASCE*, 130(9), 1006-1018.

Makris, N. and C. J. Black, 2004b. Dimensional analysis of bilinear oscillators under pulse-type excitations. *Journal of Engineering Mechanics, ASCE*, 130(9),1019-1031.

Naeim, F. and Kelly, J. M., 1999. Design of Seismic Isolated Structures; From Theory to Practice. *Wiley , Chichester*, U.K.

Park, J-G. and Otsuka, H., 1999. Optimal yield level of bilinear seismic isolation devices. *Earthquake Engineering and Structural Dynamics*, 28(9), 941-955.

Veletsos, A. S., Newmark, N. M., Chelepati, C. V., 1965. Deformation spectra for elastic and elastoplastic systems subjected to ground shock and earthquake motions. *Proc. of the 3rd World Conf. on Earthquake Engineering*, New Zealand, 2, 663-682.